利用ACA驱动的测量矩阵插值加速目标宽带电磁散射特性分析

王仲根*[①]　吴承钢[①]　聂文艳[②]　孙玉发[③]

[①](安徽理工大学电气与信息学院　淮南　232001)

[②](淮南师范学院机械与电气工程学院　淮南　232001)

[③](安徽大学电子信息工程学院　合肥　230601)

摘　要：针对目标宽带电磁散射特性分析中待求频点阻抗矩阵重复计算、矩阵方程重复求解的问题，本文提出一种基于压缩感知框架的自适应交叉近似(ACA)驱动测量矩阵插值(MMI)的高效计算方法。该方法首先在最高频率点通过ACA提取主导行索引并全频段复用，实现测量矩阵确定性构建；其次采用MMI技术，通过少量采样频点的低维测量矩阵插值避免完整阻抗矩阵冗余计算；最后对插值后矩阵的远场组再次进行ACA分解，进一步加速矩阵向量积运算，实现传感矩阵的快速构建，将电流系数求解转换成压缩感知模型下超定方程的求解，实现待求频点电流快速求解。研究结果表明，该方法在保证计算精度的前提下，有效提高了测量矩阵的构造效率，显著降低插值的矩阵维数，大幅提升了目标宽带散射分析的效率。

关键词：宽带散射；压缩感知；自适应交叉近似；测量矩阵插值

中图分类号：TN011　　**文献标识码**：A　　**文章编号**：1009-5896(2026)00-0001-08

DOI: 10.11999/JEIT260392　　**CSTR**: 32379.14.JEIT260392

1　引言

目标宽带电磁散射在雷达目标识别、隐身与反隐身技术以及微波成像等现代领域中具有重要应用价值，成为当前研究的热点。矩量法[1,2](Method of Moments, MoM)因其计算精度高而得到广泛应用。然而，当目标为电大尺寸或具有复杂几何结构时，矩量法构建与求解大规模阻抗矩阵的过程会产生过高的计算与存储开销。为了应对这一挑战，学术界开发了多种加速算法，包括快速多极子法(Fast Multipole Method, FMM)[3]、多层快速多极子方法(Multilevel Fast Multipole Method, MLFMM)[4]以及基于自适应交叉近似(Adaptive Cross Approximation, ACA)的方法[5,6]。尽管如此，在宽带分析过程中，阻抗矩阵和矩阵方程通常需要随频率变化进行逐频点重复构造和重复计算，这依然引入大量计算冗余。

为缓解宽带扫频重复计算问题，渐近波形估计(Asymptotic Waveform Evaluation, AWE)[7]、基于模型的参数估计(Model-Based Parameter Estimation, MBPE)[8]以及阻抗矩阵插值[9–11]等技术被引入宽带散射分析。其中，AWE通过频域泰勒级数展开与余项拟合实现宽带快速外推，近年来常与插值、低秩分解结合以拓展适用带宽，但仍受展开阶数与拟合精度限制，在宽频段场景下易出现误差累积；MBPE通过有理函数拟合频域响应，需预先获取多个频点电流或矩阵信息，前期采样成本较高；阻抗矩阵插值直接对频域阻抗元素进行插值逼近，无需逐频完整求解矩阵方程，成为工程中常用的宽带加速路线，然而传统阻抗矩阵插值仍需在各采样频点计算完整的高维阻抗矩阵，存储与计算开销依旧可观。

近年来，压缩感知(Compressive Sensing, CS)[12]被引入矩量法中，成为分析电磁散射问题的有效手段，即压缩感知矩量法(Compressive Sensing MoM, CS-MoM)[13]。在此基础上，结合超基函数(Hyper-Basis Functions, HBFs)与压缩感知的CS-HBFM[14]技术被提出，为宽带求解提供了新的思路。目前常用的基函数包括 Krylov子空间基函数[15]、特征基函数(Characteristic Basis Functions, CBFs)[16–18]以及特征模基函数(Characteristic Mode Basis Functions, CMBFs)[19]，CS-HBFM仅在最高频率点计算一次CMBFs，有效消除了各频点基函数的重复生成负担，同时借助CS实现了计算加速。但该方法采用的随机采样[20]和均匀采样[21]策略本质上具有非确定性。此外，其传感矩阵的构建涉及大规模矩阵向量积。更为关键的是，该方法在各频点仍需重复构建并求解阻抗矩阵方程，效率低下。

为了克服现有宽带求解方法的上述局限性，本文提出一种将CS与测量矩阵插值相结合的新型分

收稿日期：2026-04-07；改回日期：2026-06-29；网络出版：2026-07-13

*通信作者：　王仲根　zgwang@ahu.edu.cn

基金项目：国家自然科学基金(62071004)，安徽省教育厅科学研究重点项目(2025AHGXZK31006)

Foundation Items: The National Natural Science Foundation of China (62071004), The Natural Science Research Project of Anhui Educational Committee (2025AHGXZK31006)

析方法(CS-ACA-MMI)。该方法首先在最高频率点利用ACA算法提取代表主要Rao–Wilton–Glisson (RWG)基函数的行索引，并将其在全频段复用，实现测量矩阵的确定性构建，有效规避非确定性采样与重复计算问题。随后提出测量矩阵插值(Measurement Matrix Interpolation, MMI)的技术，通过直接对测量矩阵进行插值，避开完整阻抗矩阵的生成过程。最后在各频点对插值后的测量矩阵远场组进行ACA分解，将大规模矩阵向量积转化为高效的小矩阵运算。所提CS-ACA-MMI方法可显著提升宽带电磁散射问题的计算效率。

2 压缩感知结合超基函数法(CS-HBFM)

对于理想导体(PEC)目标的宽带电磁散射问题，各频点的积分方程转化为矩阵方程，从而实现任意频率$f_x \in [f_{\rm L}, f_{\rm H}]$下电流求解：

$$\boldsymbol{Z}(f_x)\boldsymbol{I}(f_x) = \boldsymbol{E}(f_x) \tag{1}$$

式中，$\boldsymbol{Z}(f_x)$表示$N\times N$的阻抗矩阵，$\boldsymbol{E}(f_x)$表示$N\times 1$的激励矩阵，$\boldsymbol{I}(f_x)$为待求解的电流系数，N为未知数的数目。在最高频率$f_{\rm H}$处构建HBFs ($\boldsymbol{J}^{\rm HBF}$)，用于表征整个频率范围内的离散电流。此时，$\boldsymbol{I}(f_x)$可以转换为如下形式：

$$\boldsymbol{I}(f_x) = \begin{bmatrix} \boldsymbol{I}(f_x)^1 \\ \vdots \\ \boldsymbol{I}(f_x)^j \\ \vdots \\ \boldsymbol{I}(f_x)^N \end{bmatrix} = \sum_{i=1}^{K} \boldsymbol{\alpha}_i \begin{bmatrix} \boldsymbol{J}_i^1 \\ \vdots \\ \boldsymbol{J}_i^j \\ \vdots \\ \boldsymbol{J}_i^N \end{bmatrix} = \boldsymbol{J}^{\rm HBF}\boldsymbol{\alpha}_K \tag{2}$$

其中$\boldsymbol{\alpha}_K$表示$K\times 1$的电流系数，将式(2)代入式(1)，可得：

$$\boldsymbol{Z}(f_x)\boldsymbol{J}^{\rm HBF}\boldsymbol{\alpha}_K = \boldsymbol{E}(f_x) \tag{3}$$

为构建CS框架，对$\boldsymbol{Z}(f_x)$和$\boldsymbol{E}(f_x)$采用随机采样策略，得到测量矩阵$\boldsymbol{Z}^{\rm M}(f_x)$和测量激励$\boldsymbol{E}^{\rm M}(f_x)$，将其代入式(3)，可得如下方程：

$$\boldsymbol{Z}^{\rm M}(f_x)\boldsymbol{J}^{\rm HBF}\boldsymbol{\alpha}_K = \boldsymbol{E}^{\rm M}(f_x) \tag{4}$$

通过上述运算，可获得传感矩阵$\boldsymbol{\Theta} = \boldsymbol{Z}^{\rm M}\boldsymbol{J}^{\rm HBF}$。最后利用最小二乘法重构电流系数$\boldsymbol{\alpha}_K$：

$$\boldsymbol{\alpha}_K = \left(\boldsymbol{\Theta}^{\rm H}\boldsymbol{\Theta}\right)^{-1}\left(\boldsymbol{\Theta}^{\rm H}\boldsymbol{E}^{\rm M}\right) \tag{5}$$

3 ACA驱动测量矩阵插值法(CS-ACA-MMI)

区别于传统的CS-HBFM[14]方法，本文提出的CS-ACA-MMI框架通过插值操作将高维的完整阻抗矩阵降至低维的测量矩阵，从根本上降低了扫频分析中的计算开销。该方法的核心逻辑在于利用双重ACA策略[5]和测量矩阵插值技术对CS全流程进行协同加速，具体而言，该算法流程由以下三个紧密衔接的部分组成：

3.1 CMBFs的构造和基于ACA的确定性行索引提取

CMBFs本质上具有频率不变量特性，能够表征目标主导模态分布的稳定性，这构成了宽带分析中基函数复用技术的底层理论基础。为实现电流展开的低秩稀疏化，本文在最高频率$f_{\rm H}$处构建阻抗矩阵，并依据模态显著性(MS)准则对CMBFs进行筛选。MS准则[19]通过定量评估各模态对总散射电流的贡献程度，从而识别出关键模态，其具体定义为：

$$\mathrm{MS} = \left|\frac{1}{1+j\lambda_i}\right| (i = 1,2,\cdots,n) \tag{6}$$

其中λ_i为特征值，通过设定合理的MS阈值$\tau_{\rm CM}$，可以剔除散射贡献较弱的次要模态，仅选取特征值满足$\lambda_i \ge \tau_{\rm CM}$的显著特征值$\lambda_i$作为HBFs。

随后，在$f_{\rm H}$处对完整阻抗矩阵进行ACA，通过低秩分解在式(7)过程中提取主导行索引r_n^m：

$$\boldsymbol{Z}(f_{\rm H}) = \boldsymbol{U}(f_{\rm H})\boldsymbol{V}(f_{\rm H}) \tag{7}$$

作为一种核无关的低秩逼近方法，ACA能够捕获矩阵内基函数间的强耦合特性，从而提取出代表主导RWG基函数的行索引。这些索引精准识别出了具有强耦合效应及显著散射贡献的“信息丰富”区域。区别于CS-HBFM中的非确定性采样，本文基于ACA的确定性低秩特征提取实现了索引r_n^m在全频段内的复用。由于最高频率下的矩阵秩涵盖了低频段的秩，所以所提取的r_n^m涵盖了完整的宽带散射特征，从而消除了每个频点重复提取索引的时间成本。ACA抽取策略的示意图如图1所示。

上述方法虽加速了单个频点的计算，但仍需在每个频点重复计算测量矩阵，存在明显冗余。为此本文提出测量矩阵插值技术，从根本上消除逐频计算冗余，并将插值对象从完整高维阻抗矩阵转为低维测量矩阵。

3.2 测量矩阵插值

首先，采用切比雪夫-洛巴托(Chebyshev-Lobatto)节点[22]选取四个采样频率点$f_p (p = 0,1,2,3)$。通过固定其中两个点为最低频率$f_{\rm L}$和最高频率$f_{\rm H}$，该方法能够充分利用频带边界点的物理信息。具体采样依据式(8)：

$$f_p = \frac{f_{\rm L}+f_{\rm H}}{2} - \frac{f_{\rm H}-f_{\rm L}}{2}\cos\left(\frac{p}{3}\pi\right) \tag{8}$$

随后，直接根据预先提取的行索引r_n^m填充各采样点f_p处的测量矩阵，从而彻底避开完整阻抗矩阵

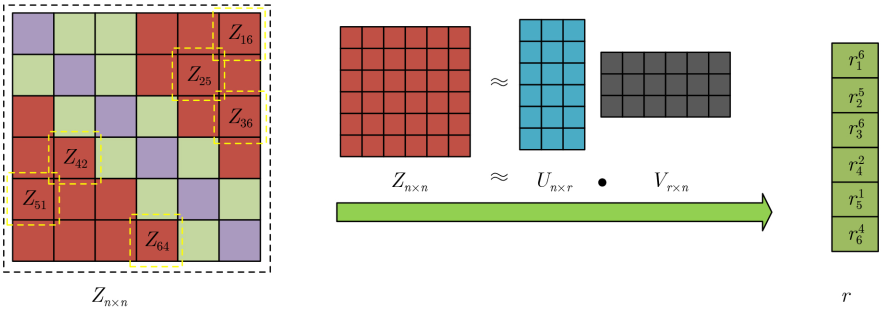

图 1 ACA测量矩阵构建示意图

的计算过程。此外，需进一步计算这四个采样点处修正后的测量阻抗元素$\tilde{z}^{\mathrm{M}}_{mn}(f_p)$[11]，其计算公式为：

$$\tilde{z}^{\mathrm{M}}_{mn}(f_p)=\left(z^{\mathrm{M}}_{mn}(f_p)f_p\right)e^{j2\pi\frac{f_p}{c}R_{mn}}/f_{\mathrm{H}} \tag{9}$$

其中，$z^{\mathrm{M}}_{mn}(f_p)$表示f_p处的真实测量阻抗元素，R_{mn}表示第m个与第n个RWG基函数中心之间的几何距离，c为自由空间中的光速。

最后，基于在采样点f_p处获得的修正测量阻抗，通过高效的插值即可得到目标频点f_x处的修正测量阻抗：

$$\tilde{z}^{\mathrm{M}}_{mn}(f_x)=\sum_{p=0}^{3}\varphi_p\tilde{z}^{\mathrm{M}}_{mn}(f_p) \tag{10}$$

其中，φ_p表示插值系数，定义为：

$$\varphi_p=\prod_{q=0,q\neq p}^{q=3}\left(\frac{f_x-f_q}{f_p-f_q}\right),(q=0,1,2,3) \tag{11}$$

由此，可以通过插值得到的修正测量阻抗还原得到对应频点的真实测量阻抗$z^{\mathrm{M}}_{mn}(f_x)$：

$$z^{\mathrm{M}}_{mn}(f_x)=\left(\tilde{z}^{\mathrm{M}}_{mn}(f_x)/f_x\right)e^{-j2\pi\frac{f}{c}R_{mn}}f_{\mathrm{H}} \tag{12}$$

3.3 传感矩阵的加速构建

在获取待求频率f_x下的测量矩阵后，为进一步提升计算效率，本文再次使用ACA算法对测量矩阵的远场组阻抗进行分解。通过该变换，将原本的大规模矩阵向量积运算转化为小维度的矩阵乘积，从而加速传感矩阵的构建。具体计算公式为：

$$\boldsymbol{Z}^{\mathrm{M}}_{ij}(f_x)=\boldsymbol{U}^{\mathrm{M}}_{ij}(f_x)\boldsymbol{V}^{\mathrm{M}}_{ij}(f_x) \tag{13}$$

远场阻抗被分解为矩阵$\boldsymbol{U}^{\mathrm{M}}_{ij}(f_x)$和$\boldsymbol{V}^{\mathrm{M}}_{ij}(f_x)$。首先将$\boldsymbol{V}^{\mathrm{M}}_{ij}(f_x)$与基函数$\boldsymbol{J}^{\mathrm{HBF}}$相乘，再与$\boldsymbol{U}^{\mathrm{M}}_{ij}(f_x)$相乘，即可构建处远场的传感矩阵。由于两个低秩矩阵的维度都是与秩相关，要远远小于测量矩阵的维度，所以能够显著提高计算效率。而近场部分，则直接通过测量矩阵与基函数相乘得到传感矩阵。最终得到的传感矩阵形式如下：

$$\boldsymbol{\Theta}=\begin{bmatrix}\boldsymbol{Z}^{\mathrm{M}}_{11}\boldsymbol{J}^{\mathrm{HBF}}_1 & \boldsymbol{Z}^{\mathrm{M}}_{12}\boldsymbol{J}^{\mathrm{HBF}}_2 & \cdots & \boldsymbol{U}_{1j}(\boldsymbol{V}_{1j}\boldsymbol{J}^{\mathrm{HBF}}_j)\\ \boldsymbol{Z}^{\mathrm{M}}_{21}\boldsymbol{J}^{\mathrm{HBF}}_1 & \boldsymbol{Z}^{\mathrm{M}}_{22}\boldsymbol{J}^{\mathrm{HBF}}_2 & \cdots & \boldsymbol{U}_{2j}(\boldsymbol{V}_{2j}\boldsymbol{J}^{\mathrm{HBF}}_j)\\ \vdots & \vdots & \ddots & \vdots\\ \boldsymbol{U}_{i1}(\boldsymbol{V}_{i1}\boldsymbol{J}^{\mathrm{HBF}}_1) & \boldsymbol{U}_{i2}(\boldsymbol{V}_{i2}\boldsymbol{J}^{\mathrm{HBF}}_2) & \cdots & \boldsymbol{Z}^{\mathrm{M}}_{ij}\boldsymbol{J}^{\mathrm{HBF}}_j\end{bmatrix} \tag{14}$$

最终，该方法将电流系数的求解从一个稠密矩阵方程转化为一个超定方程，并采用最小二乘法对电流系数进行重构，加快宽带电磁散射求解。

4　复杂度分析

在本节中，作者对比分析了CS-ACA-MMI和CS-HBFM两种方法的计算复杂度。为了方便计算，设定N为未知数的数目，K为HBFs的数量，M为CS-HBFM中随机抽取的行数，而S为CS-ACA-MMI中ACA选取的行数。由于ACA提取的行索引比随机抽取更具物理代表性，通常满足$S<M$。本次分析针对包含N_f个频点的宽带扫频过程展开，分别从测量矩阵构建与传感矩阵构建两个维度，定量分析了所提CS-ACA-MMI框架与传统CS-HBFM方法的计算复杂度。对比分析结果如表1所示，直观地体现了本文方法在计算效率上的显著优势。

4.1 测量矩阵

通过引入插值技术，原本在N_f个频率点处重复计算格林函数的冗余操作，仅需4个Chebyshev节点处的高精度插值即可。由此计算复杂度从$O(N_fMN)$降至$O(4SN)$，其中$N_f\gg4$。

表 1　两种方法的计算复杂度对比

方法	测量矩阵构建	近场传感矩阵构建	远场传感矩阵构建
CS-HBFM	$O(N_fMN)$	$O((1-\eta)N_fMNK)$	$O(\eta N_fMNK)$
CS-ACA-MMI	$O(4SN)$	$O((1-\eta)N_fSNK)$	$O(\eta N_fRNK)$

4.2 传感矩阵

ACA被应用于测量矩阵的远场组阻抗矩阵分解(远场占比为$\eta \approx 0.8$)，采用本文所提的方法，近场传感矩阵的计算复杂度由$O((1-\eta)N_f MNK)$降至$O((1-\eta)N_f SNK)$。远场复杂度从$O(\eta N_f MNK)$显著降至$O(\eta N_f R(N+S)K)$，由于$S \ll N$，S可以忽略不计，所以远场复杂度可以优化为$O(\eta N_f RNK)$，其中R为测量矩阵的有效秩。

综上所述，CS-HBFM中完整的传感矩阵构建复杂度为$O((1-\eta)N_f MNK)+O(\eta N_f MNK)$，而CS-ACA-MMI的计算复杂度为$O((1-\eta)N_f SNK)+O(\eta N_f RNK)$，由于$R \ll S < M$，所以CS-ACA-MMI的复杂度显著低于CS-HBFM。

5 数值算例

本节通过三个数值实例验证了所提算法的有效性。文中采用宽带雷达散射截面(RCS)的均方根误差(RMSE)作为精度衡量指标，其具体定义如下：

$$\mathrm{RMSE} = \sqrt{\frac{1}{N_f}\sum_{i=1}^{N_f}(\sigma_{\mathrm{cal}} - \sigma_{\mathrm{MoM}})^2} \tag{15}$$

其中，N_f为待求解点数，σ_{cal}和σ_{MoM}分别表示本文所提方法和矩量法的计算结果。

算例 1：计算了一个半径为0.2 米，高为1 米的圆柱体的宽带RCS，分析频段范围为100 MHz到1 000 MHz，步长为45 MHz。该圆柱体表面被剖分为6 670个三角单元，得到10 005个未知数。将目标划分为8个子域，每个子域向外扩展0.15倍波长，扩展后得到15 352个未知数。MS阈值设置为0.000 5，共生成833个HBFs。

为了验证ACA的物理有效性，图2展示了所提ACA策略选取行索引的空间分布，红色圆点为ACA选取的行索引位置。正视图清晰地呈现出一种非随机的、分层分布的模式，行索引在对应圆柱体子域几何交界的七个水平层上显著聚集。这表明ACA能够有效捕捉几何边界处复杂的表面电流分布，并将其识别为信息富集的“热点”区域。此外，俯视图显示圆柱体边缘处的索引分布密度极高。上述结果有力地证明了所选索引是由物理模型的几何结构决定的，从而为其在全频段内的复用提供了物理依据。

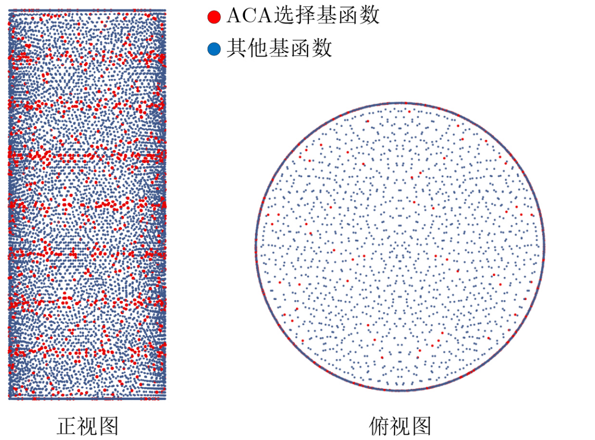

图 2 ACA全局行索引的高亮图

图3和图4分别展示了两次ACA不同阈值下的计算时间和RMSE，图中绿色的点表示最终选取的参数，选取标准是在这个点之后RMSE的增益不高，但是时间成本依旧稳定上升，所以最终设定两次ACA的阈值分别为5×10^{-7}和1×10^{-3}。

图5给出了不同采样点下计算时间和RMSE随采样点数量的变化趋势。显而易见，采用四个采样点可实现效率与精度的最优平衡，因为进一步增加采样点虽然会提升计算成本，但带来的精度增益极小。因此，本文最终选取四个频点进行测量矩阵插值。

图6给出了三种方法计算得到的宽带RCS结果。可以看出，本文所提方法与矩量法(MoM)的计算结果吻合较好。

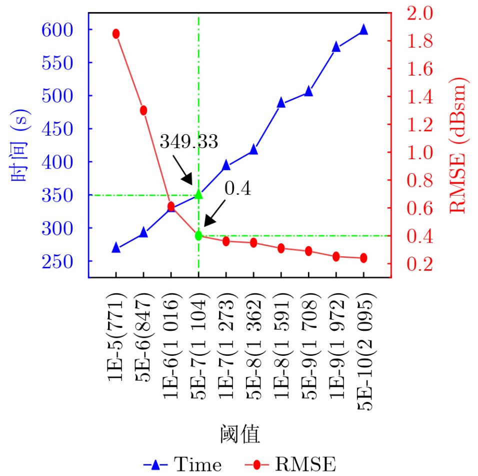

图 3 行索引获取中不同ACA阈值下的时间和RMSE

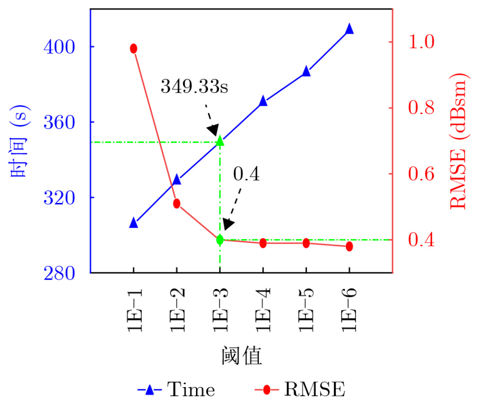

图 4 传感矩阵构建中不同ACA阈值下的时间和RMSE

算例 2：计算了一个间隙为0.7米的带缝圆锥，分析频段范围为0.3 GHz到3.5 GHz，步长为0.1 GHz。目标表面被剖分为9 072个三角面元，得到13 608个未知数。接着将目标划分为18个子域，每个子域向外扩展0.15倍波长，共得到22 264个未知数。MS的阈值设置为0.002，在最高频率点共获得1 151个HBFs。两次ACA的阈值分别设定为1×10^{-8}和1×10^{-3}。应用MoM，CS-HBFM和CS-ACA-MMI三种方法计算的RCS结果如图7所示，从图7中可以看出CS-ACA-MMI在分析复杂目标时具有良好的计算精度。

算例 3：计算了一个长度为504.748 毫米的杏仁体，分析频段范围为0.8 GHz到4 GHz，步长为80 MHz。目标表面被剖分为39 186个三角面元，得到58 779个未知数。接着将目标划分为26个子域，每个子域向外扩展0.15倍波长，共得到91 233个未知数。MS的阈值设置为0.002，在最高频率点共获得3 628个HBFs。两次ACA的阈值分别设定为1×10^{-10}和1×10^{-3}。应用MoM, CS-HBFM和CS-ACA-MMI三种方法计算的RCS结果如图8所示，从图8中可以看出两种方法的计算结果与MoM的计算结果吻合良好。

为进一步验证所提方法的计算效率，表2给出了CS-HBFM与CS-ACA-MMI抽取行数、计算时间、计算误差与内存消耗的对比。如表2所示，在保持相同精度的前提下，本文方法实现了显著加速，在三个算例中总计算时间分别缩减了93.4%、96.7%和81%。此外，单个频点测量矩阵的内存占

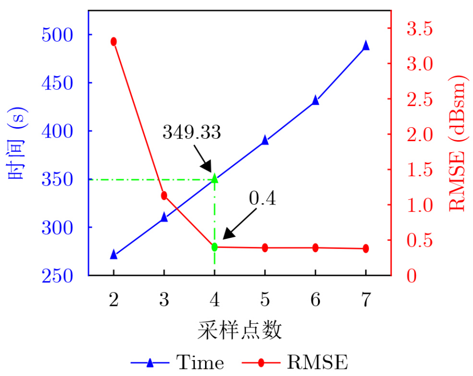

图 5 不同采样点数下的时间和RMSE

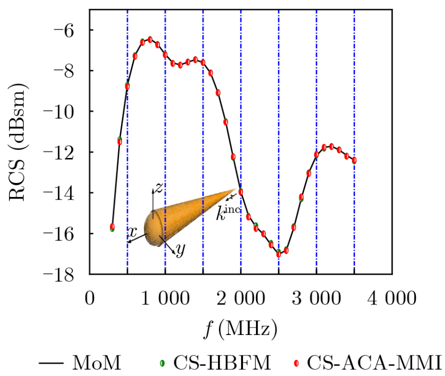

图 7 带缝圆锥的宽带RCS

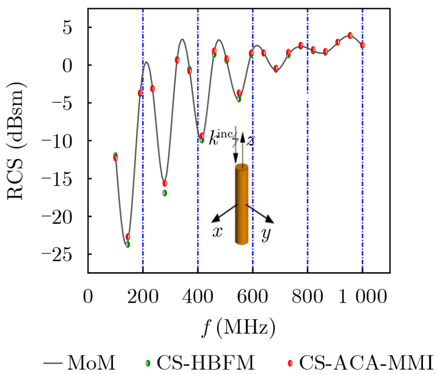

图 6 圆柱体的宽带RCS

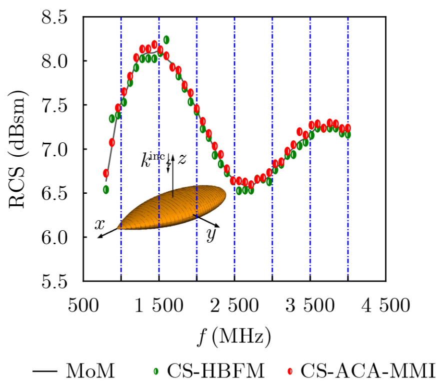

图 8 杏仁体的宽带RCS

表 2　两种方法的计算时间对比

目标	方法	抽取行数	总时间(s)	RMSE(dBsm)	单频点测量矩阵的内存(GB)
圆柱体	CS-HBFM	3 001	5 285.27	0.46	0.46
	CS-ACA-MMI	1 104	349.33	0.4	0.16
带缝圆锥	CS-HBFM	4 082	34 991.7	0.04	0.83
	CS-ACA-MMI	2 839	1 154.52	0.05	0.58
杏仁体	CS-HBFM	17 633	180 182.5	0.07	15.44
	CS-ACA-MMI	13 292	34 316.2	0.05	11.64

用量分别降低了65%、30%和25%，并且CS-ACA-MMI只需储存四个采样点的测量矩阵，而CS-HB-FM则需要每个目标频率都计算测量矩阵。

6 结论

本文提出了一种CS-ACA-MMI加速宽带电磁散射分析的有效方法。该方法在CS框架下，将ACA与MMI有效结合，有效解决了逐频点重复填充矩阵所带来的计算瓶颈。具体而言，该方法利用最高频点处的 ACA算法提取主导行索引，不仅确保了采样的确定性，还为全频段测量矩阵插值提供了稳定的基准。其次，通过对低维测量矩阵而非全阻抗矩阵进行插值，显著降低了插值的维度，并避免逐频点冗余计算。此外，通过引入二次ACA分解进一步加速了感知矩阵的构建。数值实验结果表明，与传统的CS-HBFM方法相比，CS-ACA-MMI在保持高精度的同时，加速比均超过80%。

参 考 文 献

[1] HARRINGTON R F. Field Computation by Moment Methods[M]. New York: Macmillan, 1968: 22–57.

[2] CANDES E J, ROMBERG J, and TAO T. Robust uncertainty principles: Exact signal reconstruction from highly incomplete frequency information[J]. *IEEE Transactions on Information Theory*, 2006, 52(2): 489–509. doi: 10.1109/TIT.2005.862083.

[3] 陈新蕾, 邓小乔, 李茁, 等. 金属介质混合目标散射分析的快速偶极子法[J]. 电子与信息学报, 2011, 33(11): 2790–2794. doi: 10.3724/SP.J.1146.2011.00398.

CHEN Xinlei, DENG Xiaoqiao, LI Zhuo, *et al.* Electromagnetic scattering by mixed conducting and dielectric objects analysis using fast dipole method[J]. *Journal of Electronics & Information Technology*, 2011, 33(11): 2790–2794. doi: 10.3724/SP.J.1146.2011.00398.

[4] SONG J M and CHEW W C. Multilevel fast-multipole algorithm for solving combined field integral equations of electromagnetic scattering[J]. *Microwave and Optical Technology Letters*, 1995, 10(1): 14–19. doi: 10.1002/mop.4650100107.

[5] WANG Zhonggen, DONG Dai, GUO Fei, *et al.* Fast construction of measurement matrix and sensing matrix with dual adaptive cross approximation[J]. *IEEE Antennas and Wireless Propagation Letters*, 2025, 24(1): 13–17. doi: 10.1109/LAWP.2024.3481498.

[6] FANG Xiaoxing, HELDRING A, RIUS J M, *et al.* Nested fast adaptive cross approximation algorithm for solving electromagnetic scattering problems[J]. *IEEE Transactions on Microwave Theory and Techniques*, 2020, 68(12): 4995–5003. doi: 10.1109/TMTT.2020.3024732.

[7] XU Zhou, WANG Xing, CHEN Lin, *et al.* Combination of adaptive cross approximation and asymptotic waveform evaluation for efficient analysis of wide-band RCS[J]. *IEEE Transactions on Antennas and Propagation*, 2025, 73(11): 9648–9653. doi: 10.1109/TAP.2025.3589667.

[8] WANG Xiande and WERNER D H. Improved model-based parameter estimation approach for accelerated periodic method of moments solutions with application to the analysis of convoluted frequency selected surfaces and metamaterials[J]. *IEEE Transactions on Antennas and Propagation*, 2010, 58(1): 122–131. doi: 10.1109/TAP.2009.2036196.

[9] NEWMAN E and FORRAI D. Scattering from a microstrip patch[J]. *IEEE Transactions on Antennas and Propagation*, 1987, 35(3): 245–251. doi: 10.1109/TAP.1987.1144084.

[10] LI Weidong, ZHOU Houxing, HONG Wei, *et al.* An accurate interpolation scheme with derivative term for generating mom matrices in frequency sweeps[J]. *IEEE Transactions on Antennas and Propagation*, 2009, 57(8): 2376–2385. doi: 10.1109/TAP.2009.2024476.

[11] CHEN Xinlei, ZHANG Liyang, GU Changqing, *et al.* Wideband Sherman-Morrison-Woodbury formula-based algorithm for electromagnetic scattering problems[J]. *IEEE Transactions on Antennas and Propagation*, 2023, 71(6): 5487–5492. doi: 10.1109/TAP.2023.3263627.

[12] DONOHO D L. Compressed sensing[J]. *IEEE Transactions on Information Theory*, 2006, 52(4): 1289–1306. doi: 10.1109/TIT.2006.871582.

[13] SHEN Cunjie, CAO Xinyuan, QI Qi, *et al.* Underdetermined equation model combined with improved Krylov subspace basis for solving electromagnetic scattering problems[J]. *Progress in Electromagnetics Research Letters*, 2024, 119: 79–84. doi: 10.2528/PIERL24032101.

[14] WANG Zhonggen, LI Chenwei, SUN Yufa, *et al.* Fast analysis of broadband electromagnetic scattering problems by combining hyper basis functions-based mom with compressive sensing[J]. *IEEE Journal on Multiscale and Multiphysics Computational Techniques*, 2024, 9: 84–91. doi: 10.1109/JMMCT.2024.3355976.

[15] CAO Xinyuan, CHEN Mingsheng, QI Qi, *et al.* Solving electromagnetic scattering problems by underdetermined equations and Krylov subspace[J]. *IEEE Microwave and Wireless Components Letters*, 2020, 30(6): 541–544. doi: 10.1109/LMWC.2020.2988166.

[16] 王仲根, 唐晓菀, 汪强. 应用改进的主要特征基函数快速计算目标宽角度RCS[J]. 电子与信息学报, 2018, 40(3): 573–578. doi: 10.11999/JEIT170499.

WANG Zhonggen, TANG Xiaowan and WANG Qiang. Fast calculation of wide-angel RCS of objects using improved primary characteristic basis functions[J]. *Journal of Electronics & Information Technology*, 2018, 40(3): 573–578. doi: 10.11999/JEIT170499.

[17] DU Ping, TONG Ziwen, LIN Hai, *et al*. Wideband RCS analysis of finite periodic array in the vicinity of object using modified SSED-CBFM and improved FIR[J]. *IEEE Antennas and Wireless Propagation Letters*, 2025, 24(6): 1447–1551. doi: 10.1109/LAWP.2025.3539657.

[18] OU Mingrui, SUN Yufa, and SHI Chaofan. Compressive sensing enhanced multilevel characteristic basis function method for analyzing electrically large scattering problems[J]. *IEEE Antennas and Wireless Propagation Letters*, 2024, 23(2): 593–597. doi: 10.1109/LAWP.2023.3330820.

[19] TONG Ziwen, DU Ping, and ZHENG Gang. Characteristic modes analysis of finite periodic array with object using entire domain basis function method and ACA[J]. *IEEE Antennas and Wireless Propagation Letters*, 2025, 24(5): 1149–1152. doi: 10.1109/LAWP.2025.3527927.

[20] WANG Zhonggen, NIE Wenyan, and LIN Han. Characteristic basis functions enhanced compressive sensing for solving the bistatic scattering problems of three-dimensional targets[J]. *Microwave and Optical Technology Letters*, 2020, 62(10): 3132–3138. doi: 10.1002/mop.32432.

[21] GAO Yalan, AKBAR M F, and JAWAD G N. Stabilized and fast method for compressive-sensing-based method of moments[J]. *IEEE Antennas and Wireless Propagation Letters*, 2023, 22(12): 2915–2919. doi: 10.1109/LAWP.2023.3304306.

[22] BERRIOCHOA E, CACHAFEIRO A, DÍAZ J, *et al*. A note on the rate of convergence for Chebyshev-Lobatto and Radau systems[J]. *Open Mathematics*, 2016, 14(1): 156–166. doi: 10.1515/math-2016-0015.

王仲根：男，教授，研究方向为计算电磁学、阵列信号处理.
吴承钢：男，硕士生，研究方向为计算电磁学、电磁散射等.
聂文艳：女，教授，研究方向为计算电磁学、电磁散射等.
孙玉发：男，教授，研究方向为计算电磁学、天线理论及设计等.

Accelerated Broadband Electromagnetic Scattering Analysis via ACA-Driven Measurement Matrix Interpolation

WANG Zhonggen[①]　WU Chenggang[①]　NIE Wenyan[②]　SUN Yufa[③]

[①](*College of Electrical and Information Engineering, Anhui University of Science and Technology, Huainan, Anhui* 232001, *China*)

[②](*College of Mechanical and Electrical Engineering, Huainan Normal University, Huainan* 232001, *China*)

[③](*College of Electronics and Information Engineering, Anhui University, Hefei* 230061, *China*)

Abstract:

Objective Broadband electromagnetic scattering is essential in modern fields such as radar target recognition, stealth technologies, and microwave imaging. While the Method of Moments (MoM) provides high accuracy, it incurs substantial computational costs for electrically large or complex targets due to the construction and solution of large-scale impedance matrices. Although acceleration techniques like the Multilevel Fast Multipole Method (MLFMM) and Adaptive Cross Approximation (ACA) have been developed, they still require costly per-frequency recomputations during wideband sweeps. To mitigate this redundancy, techniques such as Asymptotic Waveform Evaluation (AWE), Model-Based Parameter Estimation (MBPE), and impedance matrix interpolation have been introduced. However, AWE suffers from error accumulation in wideband scenarios, MBPE entails high initial sampling costs, and traditional matrix interpolation remains burdened by the need to compute full high-dimensional matrices at sampling points. Recently, Compressive Sensing MoM (CS-MoM) and its derivative, CS-HBFM, have offered promising wideband solutions by utilizing Hyper-Basis Functions (HBFs). By calculating Characteristic Mode Basis Functions (CMBFs) only once at the highest frequency, CS-HBFM eliminates the redundant generation of basis functions. Nevertheless, existing CS-HBFM frameworks rely on non-deterministic random or uniform sampling strategies. Furthermore, they are hindered by large-scale matrix-vector products and the persistent need to reconstruct and solve impedance equations at every frequency step.

Methods With CS as the basic framework, this study proposes the CS-ACA-MMI accelerated analysis method for broadband electromagnetic scattering, which achieves efficient calculation of broadband scattering through the collaborative acceleration of dual ACA decomposition and low-dimensional measurement matrix interpolation. The specific implementation steps are as follows: First, CMBFs are constructed at the highest frequency point, and the dominant HBFs are selecting significant modes based on the Modal Significance (MS) criterion. ACA low-rank decomposition is performed on the complete impedance matrix at this frequency point to extract deterministic row indices representing the dominant Rao–Wilton–Glisson (RWG) basis functions, which are maintained throughout the frequency sweep to avoid the problem of non-deterministic sampling. Second, Chebyshev-Lobatto nodes are selected to determine four key sampling frequency points, and the low-dimensional measurement matrix of each sampling point is directly filled based on the pre-extracted row indices, circumventing the calculation of the complete high-dimensional impedance matrix, thereby significantly reducing the computational overhead of filling the matrix element-by-element at each frequency point. The measurement impedance elements of the sampling points are corrected by geometric distance, and then the corrected measurement impedance of the target frequency point is obtained via interpolation and further restored to the real measurement impedance, eliminating the redundancy of constructing measurement matrices at each frequency point. Third, a second ACA decomposition is carried out on the far-field impedance component of the interpolated measurement matrix, converting the large-scale far-field matrix-vector product into a low-dimensional matrix product. The near-field part is directly obtained by multiplying the measurement matrix with the basis function, and finally the complete sensing matrix is rapidly assembled. Fourth, the solution of the traditional dense matrix equation is transformed into the solution of an overdetermined equation under the CS framework, and the least square method is adopted to reconstruct the current coefficient, thereby calculating the broadband Radar Cross Section (RCS) of the target, with the Root Mean Square Error (RMSE) used to measure the computational accuracy. Fifth, three typical targets (including simple regular, complex slotted, and electrically large irregular structures) such as a cylinder, a slotted cone, and an almond are selected, with different broadband analysis frequency bands and subdivision parameters set. The broadband RCS is calculated by MoM, CS-HBFM, and CS-ACA-MMI respectively, and the computational accuracy, total calculation time, and memory occupation of the single-frequency point measurement matrix of the three methods are compared and analyzed to verify the effectiveness of the proposed method.

Results and Discussions Three typical numerical examples, a PEC cylinder, a cone-sphere with a gap and a almond, are used to verify the performance of the CS-ACA-MMI method. The spatial distribution of ACA-extracted row indices shows obvious hotspot clustering at geometric boundaries and structural junctions, which confirms the physical rationality and effectiveness of the deterministic sampling strategy (Fig.2). Parametric studies demonstrate that appropriate ACA thresholds and four sampling points achieve the best balance between computational accuracy and efficiency (Fig.3, Fig.4, Fig.5). The wideband RCS results calculated by the proposed method are in excellent agreement with those from the traditional MoM over the entire frequency band (Fig.6, Fig.7, Fig8). The root-mean-square errors (RMSE) remain very low, verifying the high numerical accuracy of the method. Compared with the conventional CS-HBFM method, the CS-ACA-MMI framework reduces the total computation time by 93.4% for the cylinder, 96.7% for the cone-sphere with a gap and 81% for the almond, respectively (Table 2). The significant improvement in efficiency benefits from deterministic index reuse, low-dimensional measurement matrix interpolation, and dual ACA acceleration, which effectively alleviate the heavy computational burden in wideband frequency-sweeping analysis.

Conclusions This study successfully develops a CS acceleration framework, CS-ACA-MMI, which integrates ACA with MMI. This framework effectively addresses the bottlenecks of repetitive matrix construction and equation solving in broadband electromagnetic scattering analysis, while overcoming the non-deterministic sampling and high computational/storage overhead inherent in traditional CS-HBFM. The core advantages of CS-ACA-MMI are three-fold: First, by extracting dominant row indices via ACA at the highest frequency and reusing them across the entire band, it ensures a deterministic construction of the measurement matrix and provides a stable physical benchmark for broadband interpolation. Second, the interpolation process is shifted from high-dimensional full impedance matrices to low-dimensional measurement matrices. Combined with Chebyshev-Lobatto node technology, this eliminates the redundant matrix filling at each frequency point. Third, by applying a second ACA decomposition to the far-field components, large-scale matrix-vector products are converted into low-dimensional matrix multiplications, significantly accelerating the sensing matrix construction. Numerical results for various structures (cylinder, cone-sphere with a gap, and almond) demonstrate that CS-ACA-MMI maintains high computational accuracy consistent with the conventional MoM. Meanwhile, the proposed method reduces total computation time by over 81% and cuts single-frequency memory requirements by up to 65%. By only requiring the storage of measurement matrices at a few sampling points, it markedly reduces the overall storage overhead.

Key words: broadband scattering; compressive sensing; adaptive cross approximation; measurement matrix interpolation